

Detect-and-Avoid Maneuver Planning: Benefits of Including Route Recapture

Wei-Ching Wang*

Bay Systems Consulting Inc., Moffett Field, CA 94035, USA

M. Gilbert Wu[†] and Kevin J. Monk[‡]

NASA Ames Research Center, Moffett Field, California, 94035, USA

Development of Detect-and-avoid (DAA) systems' maneuver guidance requirements at RTCA has centered on tactical maneuvers away from the intruder. Recapturing the flight-plan route the initial maneuver is not directly taken into account by most DAA maneuver guidance algorithms. This work demonstrates potential challenges and inefficiencies that can arise in recapturing the route after resolving a conflict. Horizontal resolution trajectories for a test matrix of encounters with varying aircraft speeds and geometries are computed by minimizing either flight time or deviation to serve as a baseline. Turn directions computed from a reference DAA algorithm coupled with a pilot selection model and a second algorithm called Autoresolver (AR) are compared to these baseline resolution trajectories. Baseline results show that turning into the intruder yields favorable cost for most encounters. Additional analysis of pilot response data shows that only three-fourths of pilots' horizontal maneuvers turn into intruders, a percentage much lower than the baseline results. Improvement to a DAA guidance algorithm based on findings in this work is discussed.

Nomenclature

ACAS-Xu	=	Airborne Collision Avoidance System-Xu
AR	=	Autoresolver
ATC	=	Air Traffic Controller
CA	=	Collision Avoidance
CPA	=	Closest Point of Approach
DAA	=	Detect-and-Avoid
DAIDALUS	=	Detect and AvoID Alerting Logic for Unmanned Systems
DWC	=	DAA Well Clear
GPOPS II	=	Gauss Pseudo-Spectral Optimization Software II
HITL	=	Human-in-the-Loop
HMD	=	Horizontal Miss Distance
ICAO	=	International Civil Aviation Organization
ICAROUS	=	Independent Configurable Architecture for Reliable Operations of Unmanned Systems
MACS	=	Multi-Aircraft Control System
MOPS	=	Minimum Operational Performance Standards
RotA	=	Rules of the Air
STM	=	Surveillance and Tracking Module
SWaP	=	Size, Weight, and Power
TRM	=	Threat Resolution Module
NAS	=	National Airspace Systems
UAS	=	Unmanned Aircraft Systems
VSCS	=	Vigilant Spirit Control Station
V&V	=	Verification & Validation

*Research Engineer, Bay Systems Consulting Inc., wei-ching.wang@nasa.gov

[†]Research Engineer, Aviation Systems, AIAA member, gilbert.wu@nasa.gov

[‡]Research Engineer, Human Systems Integration Division, kevin.j.monk@nasa.gov

I. Introduction

Detect-and-avoid (DAA) systems serve a critical role for unmanned aircraft systems (UAS) to operate safely in the national airspace systems (NAS) on a regular basis. Without a pilot onboard the vehicle, UAS relies on a DAA system to maintain “well clear” with other manned aircraft [1, 2]. DAA systems compute alerts for UAS operator or pilot. The alerts are computed based on a DAA Well Clear (DWC). DAA systems also compute maneuver guidance to help the UAS operator or pilot make a decision on a conflict-avoiding maneuver. Prototype alerting and maneuver guidance (referred to as guidance in this paper) algorithms have been developed [3–6] and validated via simulations and flight tests. Simulation and flight test results from running these algorithms have supported the development of DAA requirements at RTCA*. Key operational assumptions for DAA requirements by RTCA include instrument flight rules, pilot-in-the-loop, and beyond visual line of sight operations.

Research efforts on DAA guidance algorithms at RTCA have focused on its ability to help UAS pilots select an initial maneuver away from an intruder aircraft. The DAA guidance algorithm computes ranges of heading and altitude predicted to lead to conflicts. UAS pilots make decisions to maneuver the UAS based on these ranges. The requirements are based on suggestive guidance that offers multiple maneuver options instead of a single one (which would be directive guidance) in both horizontal and vertical dimensions. Once the conflict is resolved, UAS pilots plan for a return to the mission flight plan path in their own way, using DAA guidance for situation awareness. Most of the guidance algorithms [3, 5, 6] are of a tactical nature and do not directly take into account potential challenges or cost of returning the ownership to its flight plan path afterwards. For certain encounter geometries, a UAS pilot may find the intruder aircraft blocking the way of returning the UAS to the flight plan path after the initial maneuver. For certain encounter geometries, larger turns than the edge of the conflict range computed by DAA may lead to a more efficient route recapture afterwards. While experienced UAS pilots may be able to avoid such difficulty or inefficiency with smart maneuvers, the DAA guidance algorithm can potentially predict and help pilots avoid such situations by including the route recapture segment in its guidance computation. Doing so is likely to improve the efficiency and robustness of the overall system’s performance. For operational scenarios that require automated DAA, e.g., a lost link, a directive guidance algorithm that considers the route recapture segment in its calculation may not be just desirable but essential.

This paper compares the horizontal maneuver decisions computed from two guidance algorithms for a test matrix of representative DAA encounters. Theoretically, conflict-free and route-recapturing resolution trajectories are computed based on a cost function that drives toward either minimum-time or minimum-deviation. Initial DAA maneuvers from these trajectories serve as the baseline for the “best” maneuver. Two DAA guidance algorithms were analyzed using the same test matrix, and resulting initial maneuvers are compared to the baseline. Only horizontal maneuvers are compared for their turn direction and magnitude. Horizontal maneuvers are more effective than vertical maneuvers for medium-sized UAS such as TigerShark and Shadow-B, and are more robust against non-cooperative intruders, i.e., intruders without a functioning transponder. The encounters in the test matrix cover a wide range of geometry and aircraft speeds. This coverage allows the comparison to uncover the types of encounters most likely to create challenges and inefficiencies. Actual pilot maneuvers recorded during previous human-in-the-loop (HITL) simulations are also compared.

This paper is organized as follows: Section II provides background information about the DWC and guidance. Section III describes the modeling approach, cost functions, the DAA guidance algorithms, and the test matrix of DAA encounters. Section III also describes the pilot response data collected from previous HITL simulations for comparison. Section IV presents simulation results and discuss implications. Additional discussion is given in Section V. Section VI concludes this work.

II. Background

A. DAA Well Clear and Maneuver Guidance

A DAA system consists of surveillance, alerting and guidance algorithm, display, and communication components. Surveillance components, which can be onboard the vehicle or on the ground, detect intruder aircraft and send tracks to the alerting and guidance algorithm. According to the DAA Minimum Operational Performance Standards (MOPS), DO-365A, the guidance algorithm computes suggestive guidance in the form of ranges of headings and altitudes that are predicted to lead to conflicts. A conflict is computed based on a DWC definition specifically between a UAS and an intruder aircraft. Table 1 lists the two En Route DWC definitions to be published in revision B of DO-365 in early 2021. A non-cooperative well clear definition is used for non-cooperative intruders, and a cooperative well clear definition is

*Specifically, special committee 228 working group 1 (the DAA working group).

used for cooperative intruders. Cooperative intruders are equipped with a functioning transponder [7]. The parameter h^* represents the two aircraft's current altitude difference. The time parameter τ_{mod}^* [8] is an estimate of the two aircraft's time to get within Horizontal Miss Distance (HMD*). All three parameters must fall below their respective thresholds for a well clear to be violated.

Table 1 En route DWC definitions in DO-365

Name	HMD* (ft)	τ_{mod}^* (sec)	h^* (ft)
Cooperative DWC	4000	35	450
Non-Cooperative DWC	2200	0	450

The DAA alerting structure is comprised of three alert types: preventive, corrective, and warning. A preventive alert advises the pilot to maintain the UAS's altitude maneuvers. A corrective alert advises the pilot to coordinate with Air Traffic Controller (ATC) before maneuvering. A warning alert requires immediate action from the pilot to start maneuvering to maintain DWC [9]. For certain DAA equipment such as ACAS-Xu, the warning alert is replaced by resolution advisory alerts, and its alerting is based on the cooperative DWC exclusively [10]. The look-ahead time for a DAA alert is between 1 and 2 minutes.

The DAA guidance information is shown on a DAA display, indicating the ranges of headings and altitudes UAS pilots should avoid. There is a corresponding guidance type for each alert type. Aircraft performance parameters such as turn, climb, and descent rates can be used for computing the ranges of heading and altitude. If an alert is issued, the pilot is expected to execute a maneuver by selecting a target heading or altitude outside the ranges covered by the guidance information. Figure 1 shows a typical DAA display on Vigilant Spirit [11]. The color of the icon for the intruder indicates the alert type. The horizontal as well as vertical guidance bands are shown. The yellow band stands for corrective guidance, and the red band stands for warning guidance.

The Detect and Avoid Alerting Logic for Unmanned Systems (DAIDALUS) is a reference DAA algorithm for the RTCA DAA MOPS [7]. DAIDALUS's guidance computation is based on a constant turn rate, climb and descent rate of the ownship, and constant-velocity projections of traffic aircraft [12]. This projection is a state-based "dead-reckoning" trajectory assuming both the UAS and the other aircraft will continue in their current travel direction from their current respective position with their current relative vertical and horizontal velocities [13].

The Autoresolver(AR) was developed originally for resolving loss-of-separation conflicts in a strategic way from ATC's perspective and since then has been extended to resolving DAA conflicts. One thing that distinguishes AR from DAIDALUS and ACAS-Xu is that AR computes a conflict-free trajectory that does not just maneuver the UAS away from the intruder but also reconnects it to its original flight plan. AR uses aircraft types, current aircraft location coordinates, flight plans, speeds, encounter angles, and airspace boundaries to generate a resolution trajectory. There are three possible resolution trajectories: horizontal resolution types, altitude resolution types, and speed resolution types [14]. AR's search for a solution is based on a set of expert heuristic rules and not a cost function.

In addition to the aforementioned algorithms, the Airborne Collision Avoidance System-Xu (ACAS-Xu) and Reliable Operations of Unmanned Systems (ICAROUS) are also DAA algorithms. The ACAS-Xu is an implementation that meets DAA requirements. ICAROUS is an architecture that integrates a collection of algorithms for path planning. It has the capacity to return to path in a pre-determined flight plan [15]. In this work, ICAROUS is not utilized.

B. Choice of a Horizontal DAA Maneuver

Selection of turn direction by a pilot during a conflict can be based on the minimum conflict-free turn magnitude and pilots' discretion. HITL simulations showed that pilots usually select the direction of maneuver that minimizes the required magnitude of a maneuver. For example, if the guidance information indicates a left turn of 30° or more would clear the conflict, but at the same time shows that a right turn of only 10° would also clear the conflict, a majority of



Figure 1. Vigilant Spirit display

pilots would choose to turn right [16]. Nonetheless, the actual target heading selected by pilots is usually some degrees further away from the edge of the conflict range of heading. These behaviors are captured in an RTCA DAA pilot selection model [16].

III. Methodology

This work compares the horizontal DAA maneuvers computed from 3 algorithms shown in Table 2. The trajectory optimizer minimizes the cost function along the trajectory from the initial point to the recapture point. Two cost functions are used: time and deviation. Solutions of the trajectory optimizer serve as a baseline for other algorithms to compare to. DAIDALUS-P, which is DAIDALUS coupled with a simple pilot selection model, is utilized to compute the guidance bands. AR computes a trajectory that is conflict-free and includes the recapture segment. In addition to the comparison of maneuvers computed from the 3 algorithms, pilot response data collected from HITL simulations are further analyzed for pilots' choice of turn directions and compared to the baseline.

This section is organized as follows: Subsection III.A describes the test matrix. Subsection III.B describes the formulation of the optimal control problem and the trajectory optimizer. Subsection III.C introduces DAIDALUS-P, a combination of DAIDALUS and a pilot selection model that is applied to the output of DAIDALUS to select a maneuver. Subsection III.D describes the behavior of AR. Subsection III.E describes the pilot response data from the HITL simulation.

A. Test Matrix

A test matrix is created to sample a variety of pairwise encounters. Only one intruder is considered for each encounter. It is constructed from permutation of the following independent variables, shown in Table 3. The encounter set is further analyzed with two more DAA algorithms. A total of 126 encounters are simulated. Each encounter is analyzed by either assuming a cooperative DWC or a non-cooperative DWC. Wind effect is ignored in this study.

Table 3 shows the time from ownship's initial point to recapture waypoint is set to 120 seconds, which consists of 90 seconds from the initial point to unmitigated Closest Point of Approach (CPA) and 30 seconds from CPA to the recapture point. The 90 seconds time to a conflict represents a typical DAA look-ahead time. The ownship speeds of 80 and 100 KTAS are representative of mid-sized, Group 3 UAS such as Shadow-B. Without loss of generality, an intruder's relative heading of -45° , -90° , and -135° indicates that the intruder approaches from the right, and the ownship flies north when unmitigated. Positive CPA values indicate that the ownship would pass in front of the intruder without a DAA maneuver; negative CPA values indicate that the ownship would pass behind the intruder when unmitigated. A 0 CPA indicates a direct collision without mitigation.

Furthermore, the UAS pilots would maneuver to avoid conflict by turning into or turning away from the direction from which the intruder approaches. Therefore, to look into the benefits in recapture path planning, whether the ownship "turns into" or "turns away" is also a key metric for this study.

Table 3 Test matrix parameters

Parameter Type	Values
Time from Initial Point to Recapture Waypoint	120 seconds
Ownship Speed & Intruder Speed	(100, 170), (100, 100), (100, 70), (80, 136), (80, 80), (80, 56) KTAS
Time to Unmitigated CPA	90 seconds
Intruder's Relative Heading	-45° , -90° , -135° degrees
CPA Condition	-2000, -1000, -500, 0, 500, 1000, 2000 ft

B. Trajectory Optimizer

The trajectory optimizer computes a UAS resolution trajectory from an initial point to a recapture waypoint by minimizing the cost incurred along this trajectory using Gauss Pseudo-Spectral Optimization Software II (GPOPS II) [17], a general-purpose optimal control software. In addition, optimal control was previously utilized in conflict resolution research [18]. The 2-D version of the problem is formulated in the following way. Suppose the ownship and intruder's positions are functions of time t . The ownship and intruder's initial positions are defined by:

$$(x_o(0), y_o(0)) = \left(x_o^{(i)}, y_o^{(i)} \right) \quad (1)$$

$$(x_i(0), y_i(0)) = \left(x_i^{(i)}, y_i^{(i)} \right), \quad (2)$$

where the subscripts o and i represent ownship (UAS) and intruder, respectively, and the superscript (i) represents the initial condition. The ownship and intruders' initial velocities are denoted as

$$(\dot{x}_o(0), \dot{y}_o(0)) = (0, \dot{y}_o^{(i)}) \quad (3)$$

$$(\dot{x}_i(0), \dot{y}_i(0)) = (\dot{x}_i, \dot{y}_i), \quad (4)$$

where the ownship initial velocity is towards the positive y -axis, and the intruder's velocity is a constant. Therefore, the intruder's position is a known function of time:

$$(x_i(t), y_i(t)) = (x_i^{(i)} + \dot{x}_i t, y_i^{(i)} + \dot{y}_i t), \quad (5)$$

The following constraints are applied:

1) The ownship's speed is held constant:

$$v_o = \dot{y}_o^{(i)} \quad (6)$$

2) The ownship and intruder's states must not violate the DWC at any time. For this study, both the non-cooperative DWC and cooperative DWC are analyzed.

The control variable is the ownship's heading, ψ , bounded by -90° and 90° to prevent the ownship from flying backwards.

$$\psi \in [-90, 90] \text{ degrees} \quad (7)$$

The final condition is for the ownship to reach a final position:

$$(x_o(t_f), y_o(t_f)) = (0, y_o^{(i)}). \quad (8)$$

where t_f is the ownship arrival time.

The trajectory optimizer computes a conflict-free trajectory for the UAS using a cost function. In general, the cost function depends on mission objectives like vehicle performance, fuel cost [19], airspace and environmental constraints, vehicle maneuverability, terrain impact on communication, etc. This study investigates two simple cost functions, time and deviation. Time-cost focuses on traveling from one place to another as soon as possible. It is a suitable cost function for point-to-point operations, such as cargo delivery, air taxi, etc. Whereas, deviation-cost focuses on staying on its flight plan route as closely as possible. It is reasonable for some missions such as wildfire monitoring, air quality monitoring, aerial imaging and mapping, flood inundation mapping [7], and linear infrastructure inspection [20].

One of the following 2 cost functions, denoted as Min-Time and Min-Deviation, is applied. The time-cost is given by Eq.9.

$$C = \int_0^{t_f} 1 dt. \quad (9)$$

The deviation-cost is given by Eq. 10. Quadratic deviation cost has been applied to trajectory optimization problems before [21].

$$C = \int_0^{t_f} [\psi]^2 dt. \quad (10)$$

The form of the deviation cost is certainly not unique. The selected form for this work is regarded as a reasonable choice and appears to reduce turn segments in the trajectory solution. Since the potential resolution trajectories are separated by the intruder's trajectory into two solution spaces, the trajectory optimizer is run twice per encounter: one solution for "turn into" and one solution for "turn away." The run with the least cost is selected.

C. DAIDALUS-P

Since DAIDALUS generates suggestive guidance and not directive guidance, it is paired with a pilot selection model to define an initial maneuver. This resulting maneuver selection strategy is referred to as DAIDALUS-P. The simple pilot selection model selects the least turn angle predicted by DAIDALUS's guidance to be conflict-free at encounter start time. This selection model is consistent with observed pilot maneuvers [16]. For instance, if guidance bands cover from -3° to 10° , and the ownship's ground course is 0° , DAIDALUS-P selects a left turn. An instantaneous turn is assumed for the computation of DAUDALUS guidance.

D. Autoresolver(AR)

This work focuses on using a path-stretch capability of AR, referred to as the elliptic path-stretch algorithm, that provides horizontal resolution trajectories. The elliptic path stretches, characterized by a specified delay and the vector angle of the maneuver, produce a turnout segment and turnback segment [14]. Only horizontal resolution types are explored for this research. AR's resolution trajectory is a result of grid search between path stretch angle and path stretch delay. AR will keep searching among a finite number of candidate solutions until an acceptable solution, not an optimal solution by time or deviation, is found.

E. Pilot Response Data

1. HITL Simulation Overview

Pilot response data from previous NASA HITL simulations were examined for comparison purposes. Each study recruited active-duty UAS pilot participants to perform the DAA task under different implementations of the DAA system. The first of these simulations was conducted to validate the Phase 1 MOPS for DAA displays with acceptable human performance [22]. The -90° relative heading Low SWaP encounters [23] evaluated pilot responses to non-cooperative DAA conflicts with reduced DWC definitions and alternative surveillance limitations, whereas the -135° relative heading Low SWaP encounters employed a cooperative DWC. Both of these studies applied DAIDALUS as the reference DAA algorithm. Lastly, the ACAS-Xu HITL assessed pilot performance with the ACAS-Xu DAA algorithm applied (refer to [24] for a detailed description of the sensor noise model). The primary pilot task in each study was to maintain DWC while flying along a pre-filed flight path in representative Class E airspace. Pilots were trained to comply with DAA alerting and guidance that was either integrated with the tactical mission display or presented on a standalone traffic display shown on Vigilant Spirit. Maneuvers for conflict avoidance were coordinated with a confederate ATC either before or after the initial upload, depending on the severity of the threats at first alert. The ownship configuration in the Phase 1 Verification & Validation (V&V) and ACAS-Xu HITLs modeled a large UAS (MQ-9 Reaper) with a turn rate of 2 to $3^\circ/\text{s}$, while HITL Simulation 2 modeled a small-to-medium UAS (RQ-7 Shadow) with a $7^\circ/\text{s}$ turn rate. An important consideration is that the resolutions suggested by the DAA guidance bands varied across studies due to these differences in aircraft and DAA system specifications. Pilots consistently maneuvered outside of the DAA guidance bands to maintain DWC; however, the maximum heading recommended by the DAA guidance bands at the time of each upload was not available for this assessment. Nonetheless, turn magnitude, turn direction, and the time spent deviating from the flight path (i.e., off-course time) after conflict avoidance are reported in this paper.

2. HITL Encounter Set

The encounter set ($N=231$) used for the pilot response data comparison is outlined in Table 4. To focus on the effects of intruder location relative to ownship on route recapture, encounters with head-on (-180°) that did not intersect the return path were excluded from comparisons made in this paper. Distinction of the sides an intruder can approach from is ignored. Therefore, all intruders are assumed to have negative relative headings with respect to the ownship. Intruder relative heading varied between -155° to -90° , with intruders alerting to the left and right of ownship across scenarios. Relative airspeeds ranged from 41 KTAS slower to 140 KTAS faster than ownship. Two encounters alerted while the intruder was in a climb or descent toward ownship's current altitude, while the rest of encounters remained level for the duration of the encounter. Only conflicts that were successfully resolved with one or more horizontal maneuvers in response to DAA alerting and suggestive guidance bands were examined for these comparisons. Analysis focused on encounters that were corrective at first alert, as turn recommendations are more weighted in one direction once the conflicting aircraft approaches the collision avoidance (CA) alerting volume. Intruders were designed to approach the ownship.

Table 4 HITL encounter set for pilot response data

Simulation Type	Intruder Relative Heading	Relative True Airspeed to the Ownship (KTAS)	Intruder Vertical Velocity
ACAS-Xu & Phase 1 V&V	-155°	$-25, 30\text{--}34, 50\text{--}54$	Level, Climbing/Descending
	-135°	54	Level
	-130°	59	Level
	-115°	-41	Climbing/Descending
	-90°	$0, 30\text{--}34, 40, 49, 70$	Level
Low SWaP	-90° & -135°	0-140	Level

While minimal offsets in CPA were possible when confederate "pseudo" pilots controlled some conflicting virtual traffic in real-time via the Multi-Aircraft Control System (MACS) software [25] during the Phase 1 V&V study, Vigilant Spirit simulation software enabled researchers to inject intruders on their collision course for the majority of encounters in this sample. To compare pilots' maneuvers to the baseline, these encounters are simulated using the trajectory optimizer.

IV. Results

This section presents key findings and results and is organized as follows: Subsection IV.A shows statistics and analysis on the turn direction for the encounter set. Subsection IV.B elaborates on the comparison of the Min-Time and Min-Deviation's solution to DAIDALUS-P's guidance bands and identifies intriguing encounters. Subsection IV.C

analyzes the pilot response data from HITL simulations.

A. Turn Direction for the Encounter Set

The UAS pilot executes a horizontal maneuver in an encounter in two possible fashions: "turn into" or "turn away." The percentage of the initial "turn into" maneuver for Min-Time, Min-Deviation, DAIDALUS-P, and AR is tabulated in Table 5. About 2/3 of encounters for Min-Time, Min-Deviation, and AR select "turn into." Compared to Min-Time and Min-Deviation, AR has a similar percentage of "turn into", whereas DAIDALUS-P has a lower percentage.

Table 5 Statistics of turn direction

Algorithm	% of Turn Into	% of Opposite Turn Compared to Min-Time and Min-Deviation
Min-Deviation	66 %	N/A
Min-Time	65 %	N/A
DAIDALUS-P	47 %	19 % & 19 %
AR	68 %	9 % & 10 %

Results show that the initial turn direction of a resolution trajectory is not sensitive to the cost functions as Min-Time and Min-Deviation predict the same turn direction in almost all encounters. Percentage of encounters having opposite turn directions compared to Min-Time and Min-Deviation for DAIDALUS-P is approximately twice as much as AR. For encounters where Min-Time and Min-Deviation predict "turn into," DAIDALUS-P always predicts "turn away." These encounters have lower or comparable intruder speeds with a relative intruder heading of -45° and -90° . For the encounters in which DAIDALUS-P predicts opposite turn directions, there is an average extra cost of 9% and 61% for Min-Time and Min-Deviation, respectively. The turn direction impacts the Min-Deviation much more than Min-Time. AR, on the other hand, would be more likely to have opposite turn directions for encounters with a relative intruder heading of -90° and -135° .

Figure 2a and Figure 2b show the "turn into" percentage as a function of CPA distance using non-cooperative DWC and cooperative DWC, respectively. The trend for non-cooperative and cooperative DWC is similar. The ownship tends to turn into the intruder with a negative CPA value. The percentage of "turn into" begins to drop drastically when CPA is greater than 0. AR's "turn into"'s percentage is the highest probably because AR's functionality is based on a heuristic that prefers the safer "turn into." The percentage of "turn into" of DAIDALUS-P for cooperative DWC is farther from that of the trajectory optimizer's solutions than for non-cooperative DWC because the percentage of "turn into" for Min-Time or Min-Deviation for cooperative DWC is higher. Therefore, in contrast, DAIDALUS-P's "turn into" percentage appears to be lower compared to Min-Time or Min-Deviation. In addition, for -1000, -500, and 0 ft CPA, DAIDALUS-P for cooperative DWC selects "turn into" less frequently for -90° and -45° encounters in comparison to non-cooperative DWC. Based on the general trend, "turn into" percentage is slightly higher for cooperative compared to non-cooperative DWC, probably because the cooperative DWC volume is larger and therefore harder for the "turn away" trajectory to get around.

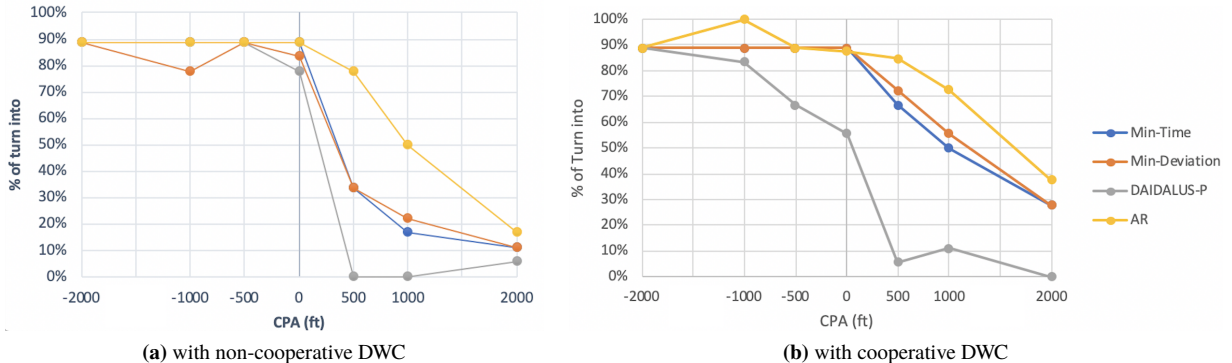


Figure 2. Percentage of "turn into" v.s. CPA distances

There are two encounters, which are about 10% of encounters that select "turn away" at -2000 ft CPA across algorithms. These two encounters have a combination of ownship speed and intruder speed of (100, 170) and (80, 156) KTAS with a relative angle of -45° encounters. Its min-time and min-deviation resolution trajectories are similar to Figure 4a in subsection IV.B.2.

B. Two Interesting Cases

This section presents two encounters that lead to interesting comparison results. Their test matrix parameters are tabulated in Table 6.

Table 6 Encounter parameters

Parameter Type	Encounter 1	Encounter 2
Ownship Speed & Intruder Speed (KTAS)	(100, 100)	(100, 170)
Cost Function	deviation	deviation
DWC	non-cooperative	cooperative
Intruder's Relative Heading (degrees)	-45	-45
CPA Condition (ft)	1000	0

1. Challenges in Route Recapture

In this category, different from the baseline, which is the trajectory optimizer that selects a "turn into" solution, DAIDALUS-P selects a "turn away" solution as shown in Figure 3a. Table A in Appendix A tabulates such encounters. Figure 3a and Figure 3b show the "turn into" and "turn away" resolution trajectories, respectively. The "turn away" trajectory has a higher cost by 63%, involves a late sharp turn. It shows an inefficient trajectory where the ownship has to pass in front of the intruder and makes a large turn to capture the recapture waypoint. The fact that the intruder slowly approaches the ownship from the side makes the trajectory risky because if the intruder turns to the left a bit, it would result in a conflict.

The baseline solution, as shown in Figure 3, is presented on the two panels. The left panel shows the ownship and intruder's trajectories and DAIDALUS's guidance bands at time zero. The right panel shows the separation between the ownship and the intruder.

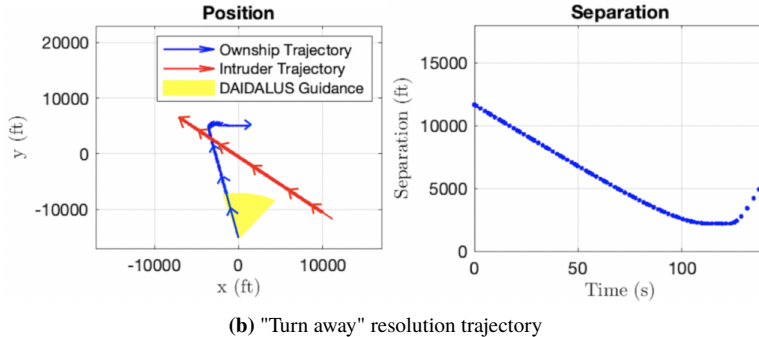
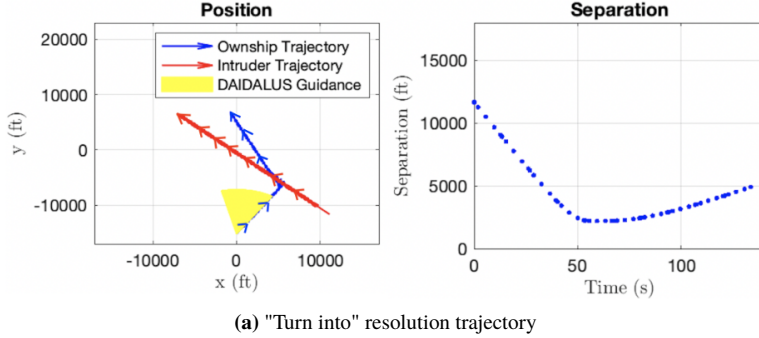


Figure 3. Challenges in Recapture

2. Baseline Turn Larger than DAIDALUS-P's Band Edge

There are 24 encounters in this category where DAIDALUS-P's bands does not cover the trajectory optimizer's initial heading. The baseline selects a "turn away" solution with an initial turn larger than indicated by the edge of DAIDALUS-P's bands. In addition, DAIDALUS-P selects the same turn direction as the baseline solution. Table B in

Appendix A shows the encounters with an ownship speed of 100 KTAS that belong to this category. It is observed that they are -45° encounters with intruder speeds faster than the ownship speeds.

Figure 4 shows the baseline resolution trajectory, in which the ownship waits for the intruder to pass in front of it. Intriguingly, the ownship's trajectory has three distinct segments. Note that DAIDALUS-P's bands cover a large part of the right turn range that discourages a "turn into." For the optimizer's resolution trajectory, a "turn away" is preferred because for an aircraft speed combination of (100, 170) and (80, 156) KTAS aforementioned in Subsection IV.A, the ownship can execute a 3-segment trajectory to pass behind the intruder. This resolution trajectory type is probably only feasible for faster intruder speeds and not found in Subsection IV.B.1.

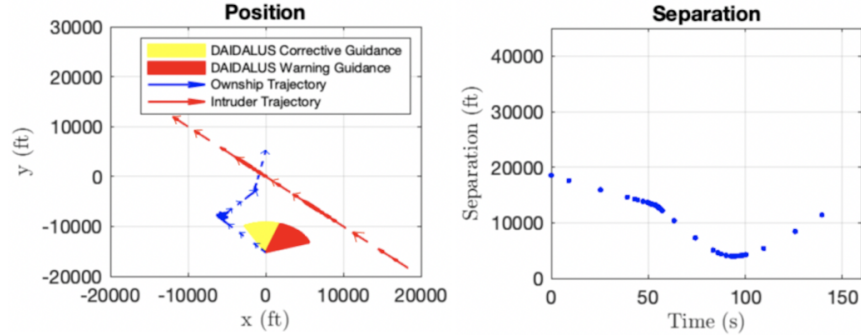


Figure 4. Wait-it-out resolution trajectory

C. Pilot Response Data

1. Turn Direction

Table 7 shows the turn direction statistics breakdown for the pilot response data. Each encounter is specified by encounter type, DWC, ownship speed, intruder speed, and relative intruder heading. Each encounter is run several times, and percentage of "turn into" is calculated accordingly from "turn into" and "turn away" count. For the three HITL experiments, ACAS-Xu, SWaP1, and Phase 1 V&V, the numbers of encounters are 68, 98, and 65, respectively. The percentage of "turn into" for ACAS-Xu, Low SWaP1, and Phase 1 V&V is calculated to be 78%, 79%, and 69%, respectively. The overall percentage of "turn into" for pilot response data is 76%. No specific trend of the percentage is observed across relative heading or speed. Nonetheless, it is observed that percentage of "turn into" is the highest for -135° and -130° intruder relative heading and -90° with identical intruder speed category.

The encounters from the pilot response data with specific aircraft speeds, relative intruder headings, and DWCS were simulated using DAIDALUS-P, Min-Time, and Min-Deviation. In the simulations, the CPA values are set to 0 ft, and time to CPA is set to 90 seconds. A 100% of "turn into" is found for Min-Time and Min-Deviation. DAIDALUS-P run selects either "turn into" or "both." The discrepancy between pilot response data's "turn into" percentage and DAIDALUS-P's could be due to the following reasons:

- 1) Pilots do not always follow the turn selection model
- 2) Small offset is in the encounter's CPA distance due to MACS
- 3) Sensor uncertainties are present in the ACAS-Xu HITL

The reason why the percentage of "turn into" is 100% for the DAIDALUS-P simulations replicating pilot response data's encounter geometries and relative aircraft speeds is that DAIDALUS-P favors a "turn into" when the intruder relative heading is less than -90° . Inspection of results in Section IV.A reveals that for DAIDALUS-P, encounters with an intruder relative heading -45° and 0 CPA distances would likely select a "turn away" solution. However, such encounters are not simulated in these HITL experiments.

2. Off-Course Time

The off-course time is estimated by the time difference between the last maneuver command upload and the initial maneuver command upload. This estimate is a bit optimistic because the route recapture does not complete until a few seconds after the last maneuver command upload is complete. The analysis focuses on a relative intruder heading of -90° , the only relative heading for which all three HITL simulations produced data.

Table 7 Turn direction statistics

Encounter Type	DWC	Ownship Speed (KTAS)	Intruder Speed (KTAS)	Relative Intruder Heading (deg)	"Turn into" count	"Turn away" count	% of "Turn into"
ACAS-Xu	Coop	197	251	-155	5	7	42%
ACAS-Xu	Coop	218	272	-155	7	2	78%
ACAS-Xu	Coop	201	176	-155	8	0	100%
ACAS-Xu	Coop	201	251	-155	5	0	100%
ACAS-Xu	Coop	218	272	-135	5	1	83%
ACAS-Xu	Coop	218	267	-90	16	2	89%
ACAS-Xu	Coop	197	246	-90	7	3	70%
Phase 1 V & V	Coop	205	235	-155	9	6	60%
Phase 1 V & V	Coop	192	226	-155	4	4	50%
Phase 1 V & V	Coop	192	251	-130	11	1	92%
Phase 1 V & V	Coop	189	148	-115	17	7	71%
Phase 1 V & V	Coop	205	245	-90	2	2	50%
Phase 1 V & V	Coop	192	226	-90	2	0	100%
Low SWaP	Coop	60	200	-135	9	0	100%
Low SWaP	Coop	100	200	-135	9	0	100%
Low SWaP	Non-Coop	100	170	-90	16	6	73%
Low SWaP	Non-Coop	100	100	-90	18	4	82%
Low SWaP	Non-Coop	60	170	-90	13	6	68%
Low SWaP	Non-Coop	60	100	-90	12	5	71%

Figure 5 shows the off-course time breakdown by HITL simulation types. "Turn into" leads to slightly less off-course time in all categories. Statistically speaking, "turn into" is likely to be more time-efficient for Low SWaP1.

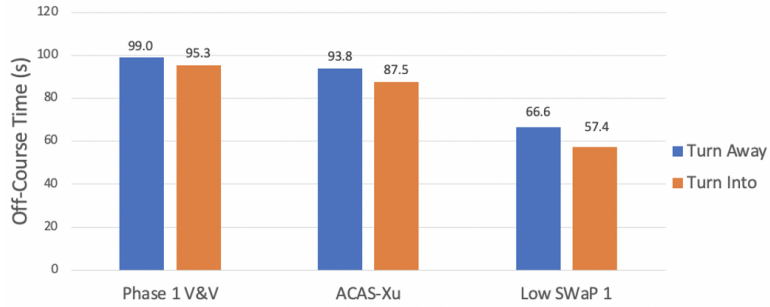


Figure 5. Off-course time breakdown

V. Discussion

Simulation results show that "turn into" is favored in most encounters in providing a minimum time cost or deviation cost resolution trajectory. For certain encounter geometries and airspeed combinations, "turn away" may lead to not just inefficiency but a challenge when trying to recapture the route. The intruder may block the ownship in its path towards a route recapture waypoint. Pilot response data indicate longer off-course time when "turn away" maneuvers are executed, highlighting the relative inefficiency of "turn away" maneuvers for certain encounters. Inspired by these findings, a potential improvement to the DAA guideline algorithm such as DAIDALUS is an addition of a preferred turn direction. This preferred turn direction can be calculated from sophisticated heuristic rules such as those in AR or from a simple look-up table that has dimensions of CPA distance and aircraft speeds and is calibrated by findings from the Min-Time or Min-Deviation resolution trajectories.

Even if DAIDALUS-P leads to the favored turn direction, the minimum-cost solution may make a turn larger than the edge of the band. This "wait-it-out" behavior is found in the Rules of the Air (RotA) specified by the International Civil Aviation Organization (ICAO). In order to pass behind the first and second hazards, the aircraft seeking to comply with the RotA is forced to perform maneuvers with the sole purpose of waiting for the other aircraft to pass [26]. It may be desirable to indicate the existence of a "wait-it-out" resolution to the UAS pilot in addition to the guidance band display in the form of a specific heading. Calculation of such a heading can be, nonetheless, a bit more advanced.

While current DAA development at RTCA assumes a pilot in the loop, in the case of a lost link, it is desirable to have an onboard DAA system capable of computing directive guidance and engaging the autopilot in executing it. For operations that go beyond the pilot-in-the-loop into automated DAA, this capability is equally essential. Such directive guidance cannot be robust unless route recapturing is taken into account. Both AR and ICAROUS plan the entire flight path all the way to the recapture point and therefore guarantee a conflict-free resolution trajectory by prediction.

VI. Conclusion

This paper investigates the benefits of including a route recapture segment in the planning of DAA maneuvers. The methodology that the trajectory optimizer, DAIDALUS-P, and AR are run using a test matrix is adapted. The trajectory optimizer providing ideal trajectories is treated as a baseline case. DAIDALUS-P, DAIDALUS coupled with a simple pilot select model, is utilized. The path stretches method for AR is introduced.

Results of DAIDALUS-P, AR, and pilot response data are analyzed and compared to that of the trajectory optimizer. Min-Time, Min-Deviation, AR, and pilot response data have the propensity of selecting a "turn into" solution. However, due to various reasons, pilot response data show more "turn away" in comparison to the algorithmic results. It can be concluded that "turn into" is favored. The trajectory optimizer's results suggest that "turn away" may cause difficulty recapturing the route when both the ownship and the intruder have comparable speeds. Besides, pilot response data show that "turn into" leads to slightly favorable off-course time. A "turn into" would be the most recommendable option unless the unmitigated CPA distance is greater than 1000 ft.

This study provides insight of DAA maneuver strategies and may have useful information for the conceptual integration of DAA guidance with an autopilot algorithm. For pilot-in-the-loop UAS operations, such insight may be applicable to the DAA guidance algorithm so as to suggest a turn direction in addition to the suggestive guidance already provided by the algorithm. Turn magnitude can be suggested as well if a wait-it-out strategy appears to be feasible and efficient.

Appendix

Table A Opposite turns between DAIDALUS-P and the trajectory optimizer

Cost Function	DWC	OWN Speed (KTAS)	INT Speed (KTAS)	INT Relative Heading (deg)	CPA Distance (ft)
Time Deviation	Non-Coop	100	70	-45	0
Time Deviation	Non-Coop	100	70	-45	500
Time, Deviation	Non-Coop	100	100	-45	500
Time, Deviation	Non-Coop	100	100	-45	1000
Time, Deviation	Non-Coop	100	170	-90	500
Time, Deviation	Coop	100	70	-90	0
Time, Deviation	Coop	100	70	-90	500
Time, Deviation	Coop	100	70	-45	0
Time, Deviation	Coop	100	70	-45	500
Time, Deviation	Coop	100	70	-45	-500
Time, Deviation	Coop	100	70	-45	1000
Time, Deviation	Coop	100	70	-45	2000
Time, Deviation	Coop	100	100	-90	500
Time, Deviation	Coop	100	100	-90	1000
Time, Deviation	Coop	100	100	-45	0
Time, Deviation	Coop	100	100	-45	500
Time, Deviation	Coop	100	100	-45	-500
Time, Deviation	Coop	100	100	-45	1000
Time, Deviation	Coop	100	100	-45	2000
Deviation	Coop	100	170	-135	500

Table B Baseline turn larger than DAIDALUS-P's band edge

Cost Function	DWC	OWN Speed (KTAS)	INT Speed (KTAS)	INT Relative Heading (deg)	CPA Distance (ft)
Deviation	Non-Coop	100	170	-45	0
Deviation	Non-Coop	100	170	-45	500
Deviation	Non-Coop	100	170	-45	-500
Deviation	Non-Coop	100	170	-45	1000
Deviation	Non-Coop	100	170	-45	-1000
Deviation	Coop	100	170	-45	0
Deviation	Coop	100	170	-45	500
Deviation	Coop	100	170	-45	-500
Deviation	Coop	100	170	-45	1000
Deviation	Coop	100	170	-45	-1000
Deviation	Coop	100	170	-45	2000
Deviation	Coop	100	170	-45	-2000

References

- [1] Cook, S. P., Brooks, D., Cole, R., Hackenberg, D., and Raska, V., "Defining Well Clear for Unmanned Aircraft Systems," *Proceedings of AIAA Infotech@ Aerospace*, AIAA, 2015. doi:<https://doi.org/10.2514/6.2015-0481>.
- [2] Johnson, M., Mueller, E. R., and Santiago, C., "Characteristics of a Well Clear Definition and Alerting Criteria for Encounters between UAS and Manned Aircraft in Class E Airspace," *Eleventh UAS/Europe Air Traffic Management Research and Development Seminar*, 2015, pp. 23–26.
- [3] Owen, M. P., Panken, A., Moss, R., Alvarez, L., and Leeper, C., "ACAS Xu: Integrated Collision Avoidance and Detect and Avoid Capability for UAS," *2019 IEEE/AIAA 38th Digital Avionics Systems Conference (DASC)*, IEEE, 2019, pp. 1–10.

[4] Abramson, M., Refai, M., and Santiago, C., “A Generic Resolution Advisor and Conflict Evaluator (GRACE) in Applications to Detect-And-Avoid (DAA) Systems of Unmanned Aircraft,” *Proceedings of the 17th AIAA Aviation Technology, Integration, and Operations (ATIO) Conference*, 2017.

[5] Muñoz, C., Narkawicz, A., Hagen, G., Upchurch, J., Dutle, A., Consiglio, M., and Chamberlain, J., “DAIDALUS: Detect and Avoid Alerting Logic for Unmanned Systems,” *34th Digital Avionics Systems Conference (DASC)*, IEEE/AIAA, 2015, pp. 5A1–1.

[6] Suarez, B., Kirk, K., and Theunissen, E., “Development, Integration and Testing of a Stand-Alone CDTI with Conflict Probing Support,” *Infotech@ Aerospace 2012*, 2012, p. 2487. doi:10.2514/6.2012-2487, URL <https://arc.aiaa.org/doi/abs/10.2514/6.2012-2487>.

[7] Wu, M. G., Lee, S., Serres, C. C., Gill, B., Edwards, M. W. M., Smearcheck, S., Adami, T., and Calhoun, S., “Detect-and-Avoid Closed-Loop Evaluation of Noncooperative Well Clear Definitions,” 2019. URL <https://doi.org/10.2514/1.D0199>.

[8] Wu, M. G., Bageshwar, V. L., and Euteneuer, E. A., “An Alternative Time Metric to Modified Tau for Unmanned Aircraft System Detect And Avoid,” *17th AIAA Aviation Technology, Integration, and Operations Conference*, 2017.

[9] Wu, M. G., Cone, A. C., and Lee, S., “Detect and Avoid Alerting Performance with Limited Surveillance Volume for Non-Cooperative Aircraft,” 2019. URL <https://doi.org/10.2514/6.2019-2073.c1>.

[10] Owen, M. P., Panken, A., Robert, M., Alvarez, L., and Leeper, C., “ACAS Xu: Integrated Collision Avoidance and Detect and Avoid Capability for UAS,” Tech. rep., Lincoln Laboratory Massachusetts Institute of Technology, Lexington, MA, 2020.

[11] Feitshans, G. L., Rowe, A. J., Davis, J. E., and Holland M. and Berger, L., “Vigilant Spirit Control Station (VSCS)—‘The face of COUNTER’,” 2018.

[12] *Minimum Operational Performance Standards (MOPS) for Detect and Avoid (DAA) Systems*, DO-365, RTCA. Inc., 2017.

[13] Cone, A. C., Wu, M. G., and Lee, S., “Detect-and-Avoid Alerting Performance for High-Speed UAS and Non-Cooperative Aircraft,” 2019. URL <https://core.ac.uk/download/pdf/227726685.pdf>.

[14] Erzberger, H., Lauderdale, T. A., Robert, M., and Chu, Y.-C., “Automated conflict resolution, arrival management, and weather avoidance for air traffic management,” Tech. rep., 2011.

[15] Consiglio, M., and Balachandran, S., “Sense and Avoid Characterization of the Independent Configurable Architecture for Reliable Operations of Unmanned Systems,” 2019.

[16] Guendel, R., Kuffner, M., and Maki, D., “A Model of Unmanned Aircraft Pilot Detect and Avoid Maneuver Decisions,” Tech. rep., MIT Lincoln Laboratory, Lexington, Massachusetts, 2017.

[17] Patterson, M. A., and Rao, A. V., “GPOPS-II: A MATLAB software for solving multiple-phase optimal control problems using hp-adaptive Gaussian quadrature collocation methods and sparse nonlinear programming,” *ACM Transactions on Mathematical Software (TOMS)*, Vol. 41, No. 1, 2014, pp. 1–37.

[18] Paielli, R. A., “Modeling Maneuver Dynamics in Air Traffic Conflict Resolution,” 2020.

[19] Wu, M. G., and Sadovsky, A. V., “Minimum-Cost Aircraft Descent Trajectories with a Constrained Altitude Profile,” Tech. rep., 2015.

[20] Bruggemann, T. S., Ford, J. J., and Walker, R. A., “Control of Aircraft for Inspection of Linear Infrastructure,” Tech. rep., 2015.

[21] Bruggemann, T. S., and Ford, J. J., “Compensation of Unmodeled Aircraft Dynamics in Airborne Inspection of Linear Infrastructure Assets,” 2011.

[22] Rorie, R., Fern, L., Monk, K., Roberts, Z., Santiago, C., and Shively, R., “Validation of Minimum Display Requirements for a UAS Detect and Avoid System,” 2017.

[23] Monk, K., Rorie, R., Keeler, J. N., and Sadler, G. G., “An Examination of Two Non-Cooperative Detect and Avoid Well Clear Definitions,” 2017.

[24] Rorie, R., Smith, C., Sadler, K., G. and Monk, Tyson, T., and Keeler, J., “A Human-in-the-Loop Evaluation of the Unmanned Aircraft System Variant of the Airborne Collision Avoidance System,” 2020.

[25] Mercer, J., Prevôt, T., Jacoby, R., Globus, A., and Homola, J., “Studying NextGen Concepts with the Multi-Aircraft Control System,” 2008.

[26] Molloy, T. L., Fulton, N. L., Garden, G. S., Williams, B. P., and Miserole, C., “Evaluation of the Rules of the Air for the Future of Air Traffic Management,” 2020.